Journal of Human-Centered Design for Manufacturing (2025), 1, 1, 25–45

doi:10.xxx.xxx/xxx

THE DESIGN ONE

ARTICLE

Multi Objective Based Cuckoo Search Algorithm Optimized PID Controller for Frequency Regulation of Interconnected Power System

Boopathi Dhanasekaran,[*†] Jagatheesan Kaliannan,[‡] Sourav Samanta,[¶] Anand Baskaran,[§] and Kanendra Naidu[|0]

†Department of Electrical and Electronics Engineering, Paavai Engineering College, Namakkal, Tamil Nadu, India
‡2Department of Electronics and Communication Engineering, M. Kumarasamy College of Engineering, Karur, Tamil Nadu, India
¶Department of Computer Science and Engineering, University Institute of Technology, The University of Burdwan, Burdwan, West Bengal, India.
§Department of Electronics and Instrumentation Engineering, Hindusthan College of Engineering and Technology, Coimbatore, Tamil Nadu, India
|0School of Electrical Engineering, Universiti Teknologi MARA, Shah Alam, Malaysia
*Corresponding author. Email: boopathime@gmail.com

Abstract

A mathematical model of an interlinked nuclear power system is investigated, and the performance of the projected algorithm is analysed in this article. A two-area nuclear power network is designed and examined for frequency regulation. Unexpected load demand is the major cause of system frequency deviation. The load frequency control (LFC) scheme is presented to the power system to control and monitor frequency deviation. The deviation can be controlled and monitored by using a secondary controller. A proportional integral derivative (PID) controller is suggested as a subordinate loop control. The cuckoo search (CS) method optimizes the controller parameters with error functions to improve the controller's performance. Four different objective functions (IAE, ITAE, ISE, and ITSE) are used in various combinations (such as single objective, double objective and mul-tiobjective functions). The simulation result evaluation effectively revealed that the multiobjective function-based CS provided a better transient response to con-trol the frequency oscillation.

Keywords: Automatic frequency control, Cuckoo search, Optimization technique, Multi-objective functions, Secondary control loop, System stability.

1. Introduction

Increasing electrical power demand and environmental degradation due to pollution from conventional power plant exhaust are major threats to the world. To equilibrium the power demand, the power plants are interconnected, and sizing is increasing. The interconnected power network has many working areas. The interconnected system has many technical issues, like frequency deviation and tie-line power flow fluctuations. The unexpected load change in the grid harms the grid and consumers. The system frequency and power should be within standard values and permissible fluctuation.

Every power system possesses several common stability control components. Every power system comprises three control loops: main, secondary, and tertiary control loops. The secondary control is done by Automatic Generation Control (AGC) or LFC methods. The important task of the AGC/LFC is to sustain the system frequency and balance the load between interconnected areas (Elgerd 1982,Elkasem et al. 2024, Younis et al. 2024,Khamies et al. 2020). Several researchers have considered this problem and tried to solve it using secondary controllers and optimization techniques.

A sliding mode controller with an event-triggering mechanism controlled a microgrid frequency oscillation. The proposed method was better than the literature results (Dev et al. 2023). PSO & GA method optimized PID controller is utilized in two-area thermal system. The efficiency of the PSO is verified with a robust test, the PSO – PID controller has reduced the system oscillation quicker than GA (Qu, Younis, Liu, et al. 2024). Particle Swarm Optimization (PSO)–Artificial Hummingbird Algorithm-based PID controller developed to maintain the system permanence of a multiple source single area power system. Thermal, wind, solar, and energy storage units (ESUs) are used to construct the system. The response was contrasted using PSO-based and traditional PID controllers (Younis et al. 2024). A qualified response analysis of LFC in an interlinked thermal power plant is illustrated (Naidu et al. 2014). Three types of Firefly Algorithm (FA) named standard, weighted, and chaotic utilized to tune PID controller gain parameters. In this comparison chaotic FA is performed better than the other two methods of FA.

Harris Hawks optimization tuned Model Predictive Controller (MPC) has been implemented for an interconnected power network (Kumar, Sharma, and Kumar 2021). A power network includes thermal and hydro as common to both areas, dish-Stirling solar thermal system and nuclear power plant included in areas 1 and 2 respectively. the anti-windup PI controller is used for LFC (Gashti and Akbarimajd 2020). An isolated nuclear power plant with ESU (capacitive energy storage) investigated for LFC using the Jaya optimization technique tuned PID controller. The ACO – PID result was compared, which is already published (Paliwal et al. 2021). An isolated nuclear power plant is inspected by ACO – PID for LFC. The study includes a response comparison of conventional PID controllers with different cost functions, at the conclusion the ACO – PID controller with ITAE is performed superior to other cost functions (Dhanasekaran, Siddhan, and Kaliannan 2020). A microgrid developed in MATLAB Simulink and examined by Teaching Learning - Based Optimization (TLBO) method-based SMC for LFC. The results of Salp Swarm algorithm (SSA), Grey Wolf Optimization (GWO), and PSO algorithms tuned SMC for supremacy of the TLBO method (Dev et al. 2024).

The PSO-PID controller was employed to analyze an autonomous power system that contained multiple sources (Qu, Younis, Wang, et al. 2024). The paper demonstrated that the PSO technique's efficacy is evaluated by altering various parameter values. A single-area nuclear power plant was investigated by a Cohort optimizer-based PID controller for LFC (Murugesan et al. 2023). The results of conventional, PSO, and Ziegler Nichols methods, the ACO technique provided better results over other methods. The efficacy of various energy storage units to LFC within an interconnected nuclear power system has been examined (Boopathi et al. 2023). ACO – PID controller is suggested for LFC. Squid game optimizer tuned Fractional order cascade controller (FOI-FOPIDD) to control the frequency damping in a two-area power network. The proposed controller result is compared with JFO, GWO, and FA (Ye et al. 2024). A two–area power network constructed with thermal, wind and PV power sources is considered for investigation of LFC. The ANFIS control is trained by an Antlion optimizer (ALO), and the investigation is conducted with different loading conditions (Fathy and Kassem 2019). The author (Namdeo, Pandit, and Paliwal 2023), investigated a standalone nuclear power plant for LFC with the support of a Sine Cosine Algorithm (SCA) tuned Fractional - PID (FOPID) controller. The classical PID and SCA–PID controller responses have been compared.

Squirrel search optimizer optimized fuzzy FOPID controller assigned for LFC in two area power networks including thermal, gas, and hydro sources. The proposed controller was evaluated against the performance of conventional PID and fuzzy PID controllers (Kalyan et al. 2023). An equal two-area power network has thermal, hydro, and gas (THG) power plants examined by the FA–PID controller for AGC. The response was compared with classical and Differential Evolution (DE) method-based PID controllers' results(Mishra, Mohanty, and Ray 2023). PV integrated two area thermal power systems that were studied using a PID controller for AGC that was optimized using the flower pollination algorithm (FPA). The FPA method's advantage was demonstrated using the GA and PSO techniques (Masikana et al. 2024). An Imperialist Competitive Algorithm (ICA) optimized Tilt FOPID controller designed for a grid-connected microgrid as a secondary controller. Microgrid formed with two area one is thermal – PV, and the other thermal – wind, both areas had ESUs (Amir et al. 2024). A PID secondary controller intended for an area thermal power network. PSO and GA, the PSO approach, are employed to enhance controller performance by optimizing gain settings (Kumar, Gupta, and Bindal 2024). Modified Cheetah Optimizer (MCO) tuned FOPID controller assigned to control the frequency oscillation in the interconnected area is structured as thermal–PV, thermal–wind, and PV–thermal. The proposed controller result has been validated with Modified Hunger Games Search Optimizer, Aquila Optimal Search, Cheetah Optimizer, and GWO-tuned FOPID controller, weighted sum-based GWO technique implemented in PID controller for LFC of two–area thermal power system (Fathy, Bouaouda, and Hashim 2024). The dominance of the proposed method is proved by comparing the result with differential evolution, Nelder-Mead simplex elephant herding optimization, membrane computing, and Luus-Jaakola algorithms (Krishna et al. 2022) and (Mamta et al. 2024). Multi-objective (MO) optimization-based GA–PI controller investigated a thermal power system for LFC (Krishna et al. 2022). A microgrid formed with diesel, wind, PV, and ESUs (BEES and FC). MO-based Artificial Rabbits Optimization (ARO) tuned PID controller (Daneshfar and Bevrani 2012), FOPID, and cascade controller (Khalil et al. 2023) were employed as a secondary controller, and various objective functions results were compared. Multi-Verse Optimizer (MVO) based MPC implemented into a multiple-area power system for LFC. The performance of the MVO with/without SMES (Khalil et al. 2024).

An FPID controller was improved using the Harmony Search - Cuckoo Optimizer (HS-CO) used in the LFC of linked power networks (Ali et al. 2020). The results of the BFOA – PID & FPID and HSCOA – PID controllers were compared in this study to prove the supremacy of the proposed method. The detailed review is reported in Table 1. The Atom Search Algorithm with PSO-tuned PID controller is suggested for conventional thermal power system (Zhao et al. 2021). Improved Weed Algorithm used to tune a PID controller for DC motor speed control test (Misaghi and Yaghoobi 2019. The literature review concludes that different researchers utilized different optimization methods to optimize the secondary controller. The PID controller is typically used as a backup controller. (Dhanasekaran, Siddhan, and Kaliannan 2020, Murugesan et al. 2023, Namdeo, Pandit, and Paliwal 2023 analyzed the single area nuclear power plant, (Namdeo, Pandit, and Paliwal 2023) analyzed interconnected nuclear power plants, and Gashti and Akbarimajd 2020, Paliwal et al. 2021, Ye et al. 2024 incorporated the nuclear power plant with conventional power sources like thermal, hydro, and gas. As discussed at the beginning of the introduction the shortage of fossil fuels and conventional sources of pollution forces people to change the sources of power production. Renewable energy sources can't compensate for the power demand, so another source has less pollution, and mass production like nuclear, is the only way. Because of this cause in this paper interconnected nuclear power plants are designed for LFC/AGC investigation.

More production capacity is needed globally to meet the growing energy demands of many countries and to replace outmoded fossil fuel facilities, especially those that burn coal and emit massive amounts of carbon dioxide into the sky. In 2022, fossil fuel combustion accounted for 61% of the power produced. Despite the significant support and expansion of intermittent renewable electricity sources in recent years (66.5% in 2005), the proportion of fossil fuels in power generation has not changed significantly over the past 15 years. Key features of nuclear power plants are as follows: (OECD International Energy Agency 2023)

- Nuclear power plants are the world's second low-carbon power production source.
- 9% of total electricity production in the world is from around 440 nuclear reactors in the world.
- The first commercial nuclear power plant was operated in the 1950s.
- In 2023, 2602 TWh of power was supplied by nuclear power plants throughout the world.
- The USA is a country that is a major utilizer of nuclear power for electricity production.

1.1 Contribution of the work

- A sophisticated, networked nuclear power plant built to evaluate the suggested controller's effectiveness against frequency deviation.
- The famous secondary controller (PID) is incorporated with the designed power system.
- Cuckoo Search Optimizer utilized to improve the controller reaction for system frequency deviation.
- Performance of the CS algorithm is tested with various objective functions with different combinations.

1.2 Construction of the paper

This article is constructed with five major sections. Section 1 is about the introduction of LFC and a detailed literature review. Section 2 covered the transfer functions and the mathematical model of the power system under investigation. Controller design and selection of fitness functions are explained in Section 3. Section 4, explains the optimization technique that is implemented to optimize the controller gain parameters and optimized controller gain values. Results of the proposed controller and result comparisons of different cost functions are reported in Section 5 in detail. Followed by section 5, the conclusion of the work is given in section 6.

Table 1. Summary of literature review.

Ref	Optimization Algorithm	Controller	Size and Source	Work
Qu, Younis, Liu, et al. 2024	PSO	PID	Two area – Thermal	The results compared with GA.
Naidu et al. 2014	Chaotic FA	PID	Two area – Thermal	Response of FA and a weighted sum of FA
Paliwal et al. 2021	Jaya optimization	PID	Single area – Nuclear with capacitive energy storage unit	ACO – PID controller result compared
Dhanasekaran, Siddhan, and Kaliannan 2020	ACO	PID	Single area – Nuclear	Conventional PID controller results and different cost function results compared
Dev et al. 2024	TLBO	SMC	Microgrid	SSA, PSO, and GWO technique tuned SMC
Qu, Younis, Wang, et al. 2024	PSO	PID	Single area – THG	Td parameters varied and the response compared
Murugesan et al. 2023	Cohort intelligence optimization	PID	Single area - Nuclear	conventional, PSO and Ziegler Nichols tuned PID controllers results compared.
Boopathi et al. 2023	ACO	PID	Two area – Nuclear	Impact of energy storage units analyzed.
Namdeo, Pandit, and Paliwal 2023	Sine cosine algorithm	FOPID	Isolated Nuclear plant	Classical PID and SCA – PID controller results compared.
Kalyan et al. 2023	Squirrel search optimizer	Fuzzy FOPID	Two area – THG	Classical PID and Fuzzy PID results compared
Mishra, Mohanty, and Ray 2023	FA	PID	Two area – THG	Classical and DE – PID controller results compared
Masikana et al. 2024	FPA	PID	Two area – PV included Thermal plant	GA and PSO methods result compared with FPA
Kumar, Gupta, and Bindal 2024	PSO	PID	Two area – Thermal	GA – PID result compared
Fathy, Bouaouda, and Hashim 2024	Modified Cheetah Optimizer	FOPID	Three area – Thermal, PV, and Wind	Modified Hunger Games Search Optimizer, Aquila Optimal Search, Cheetah Optimizer, and GWO-based FOPID controllers result compared.
Mamta et al. 2024 and Kumar, Gupta, and Bindal 2024	GWO with the weighted sum of objective	PID	Two area – Thermal	The results of differential evolution, Nelder-Mead simplex elephant herding optimization, membrane computing, and Luus-Jaakola algorithms compared.
Daneshfar and Bevrani 2012	Multi-objective function-based GA	PI	Three area – thermal	Robust test conducted
Khalil et al. 2023 and Khalil et al. 2024	Multi-Objective function–based ARO	PID, FOPID	Microgrid – Diesel, wind, PV, ESUs	Results of different objective functions compared
Ali et al. 2020	MVO	MPC	Six area – Thermal, diesel, PV, and wind	Impact of SMES is analyzed

2. Mathematical Model for Investigation

In this article, an interconnected nuclear power system is considered for the investigation of LFC. A graphical representation of the work is shown in Figure 1. The Simulink model of the investigation system is shown in Figure 3 (Murugesan et al. 2023 and Boopathi et al. 2023). As discussed earlier, the investigated system was constructed by interconnected two nuclear power plants with a grid line. The two areas are identical. Regarding the necessity of modeling the nuclear power system for LFC, the turbine, speed governor, and load should be represented.

One high-pressure (HP) turbine and two low-pressure (LP) turbines with a hydraulic amplifier make up each nuclear power station. The hydraulic amplifier must change the input to the turbine according to the control signal. The LP turbine is reached when the HP exhausts the Moisture Separator Reheater (MSR). By lowering the steam's moisture content before it enters the LP section, the MSR lowers the rates of erosion and moisture (Metwally et al. 2024). An isolated mathematical model of a nuclear plant is seen in Figure 2. Where K_h, K_g are the coefficients of HP and LP steam turbines. T_{rh} is the time constant of the LP turbine, and T1 is the HP turbine time constant.

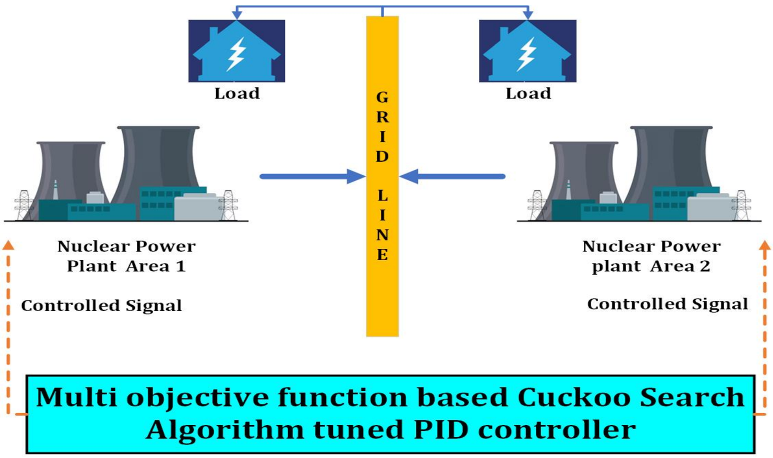

Figure 1. Pictorial representation of the mathematical model.

3. Secondary Control Loop

The PID controller for AGC is a highly regarded and extensively used controller, as evidenced by an analysis of the literature. It is stable and responds quickly in grid-connected power systems. The most popular industrial-based controller is the PID controller. Three distinct controllers were used in its construction: proportional, integral, and derivative. Each proportional controller assigned to a specific job stabilizes the gain; nevertheless, it also produces a steady-state inaccuracy. The integrated controller reduces or eliminates the mistake. The peaks are diminished by utilizing the derivative controller.

Three terms make up the output signal that the PID controller generates: one is proportional to the error signal, one is proportional to the error signal's integral, and the third is

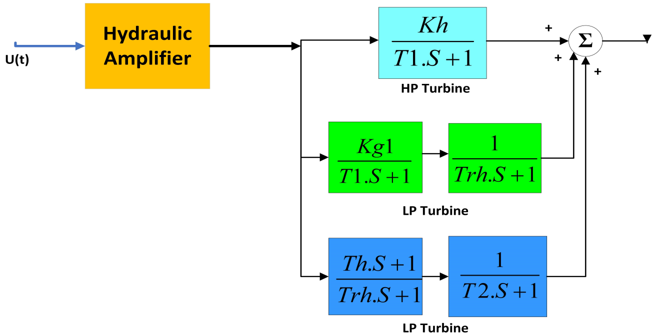

Figure 2. Mathematical model of an isolated nuclear power plant.

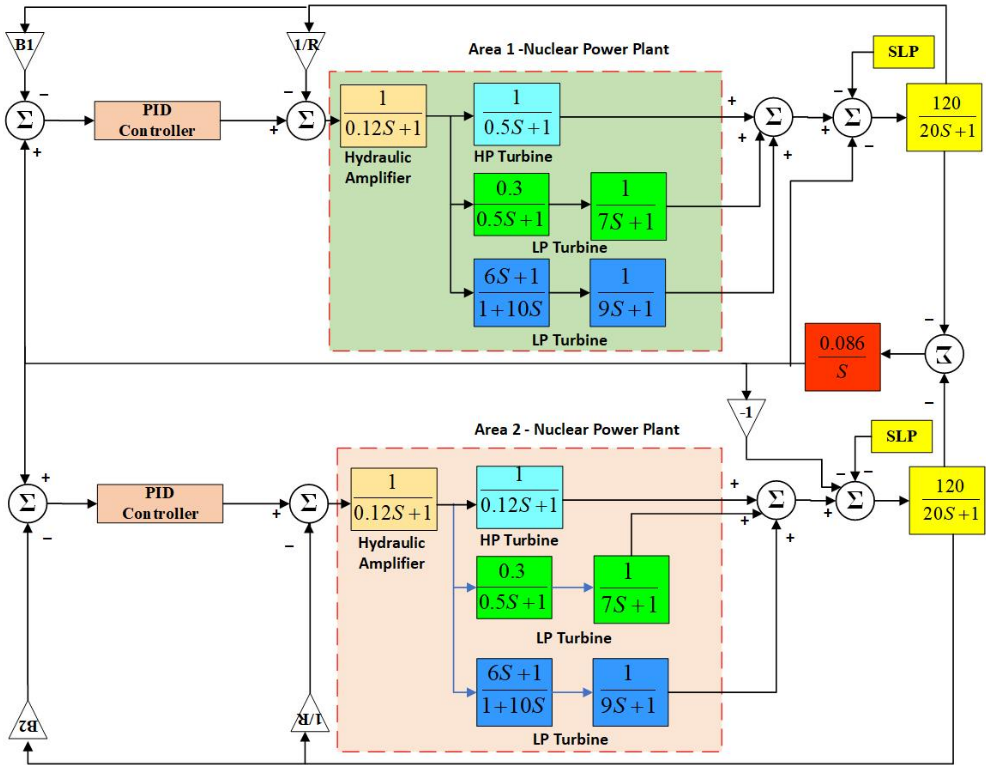

Figure 3. Simulink model of investigation power network.

proportional to the error signal's derivative.

$$u(t) \propto \alpha\left[e(t) + \int e(t)dt + \frac{d}{dt}e(t)\right],$$

$$u(t) = K_p\, e(t) + \frac{K_p}{T_i}\int e(t)\, dt + K_p\, T_d\, \frac{d}{dt}e(t), \tag{1}$$

where,

K_p = Proportional gain.
T_i = Integral time.
T_d = Derivative time.
$u(t)$ = Control signal from PID controller.
$e(t)$ = Error signal.

Take Laplace transform on both sides of equation (1).

$$U(S) = K_p E(S) + \frac{K_p}{T_i}\left(\frac{E(S)}{S}\right) + K_p T_d s E(S), \tag{2}$$

$$\frac{U(S)}{E(S)} = K_p\left[1 + \frac{1}{T_i s} + T_d s\right]. \tag{3}$$

Equation (2) represents the PID controller's output for input E (S), and equation (3) represents the PID controller's transfer function. Figure 4 displays a typical PID controller block diagram.

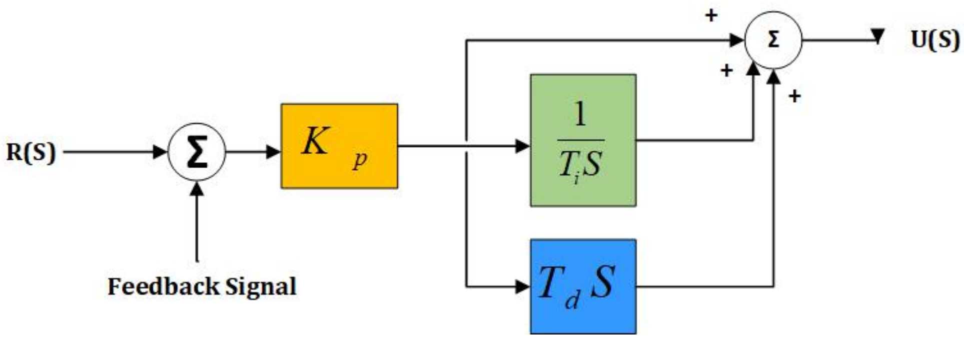

Figure 4. Typical structure of PID controller.

4. Computation Method

In the proposed work the PID controller parameters are optimized by the cuckoo search optimization algorithm while finding optimal values multi-objective function used to reduce the steady-state error.

4.1 Cuckoo Search Optimization Algorithm

The innate behavior of cuckoo animals has motivated academics to create the Cuckoo Search Algorithm for addressing optimization challenges. Yang and Deb introduced this metaheuristic approach in 2010 (Yang and Deb 2010b). Eggs are laid in other birds' nests by Cuckoos, who display obligatory brood parasitism. At regular intervals, a cuckoo hen flies down to the host's nest to lay an egg. During the breeding season, a female cuckoo may visit up to 50 nests, and this process takes about 10 seconds per nest. The host bird inspects the eggs to determine if they are its own. It may discard the alien egg or leave the nest if it detects one.

Cuckoo eggs often mimic the appearance of the host bird's eggs (Yang and Deb 2010a), making it harder for the host to detect them. The eggs typically hatch earlier than the host's eggs, causing the cuckoo chick to dislodge the host's offspring from the nest. Since the cuckoo chick is larger than the host's chicks, it monopolizes the food provided by the host's parents. Cuckoo chicks may also push other eggs or chicks out of the nest. The host's chicks will behave in the same way, forcing other birds out of the nest, if their eggs hatch before the cuckoo's.

Levy Flights

In the Cuckoo Search (CS) algorithm, both global and local search play crucial roles. These can be effectively achieved with the help of Levy flights (Yang and Deb 2013). A Levy flight is a random walk process characterized by a probability density function that includes instantaneous jumps, producing a power-law tail. This process helps the cuckoo demonstrate an optimal random search, as observed in nature (Basu and Chowdhury 2013).

Whenever a new egg is generated, Levy flights begin to guide the search toward a new location based on a randomly selected egg. During this process, if the value of the objective function at the new location is superior to that of the selected egg, the search shifts to the new position. In the case of CS, the probability of abandonment (Pa) is represented as a fraction of nests, which gives this algorithm a significant advantage over others. Each optimum in the design space is explored through Levy flight-based search, and its effectiveness has been demonstrated by comparing it to other algorithms (El-Fergany and Abdelaziz 2014).

Cuckoo Search Application To apply the Cuckoo Search algorithm, three approximation rules are followed:

1. Only one fake cuckoo egg is laid at a time, and it selects a random nest to deposit its egg in.
2. The superior quality egg is conveyed to the subsequent generation by elitist selection.
3. We provide the number of possible host nests with a probability $P_a \in [0, 1]$. The host bird will commit to eliminating the cuckoo invader if it finds a foreign egg and either discards it or leaves the nest.

The last assumption is estimated and n nests are traded for fresh nests based on the factor P_a. The objective function determines how well the solution performs. Levy flights are applied during the generation of new solutions, as described below:

$$x_i^{(t+1)} = x_i^t + \alpha \oplus Levy(\lambda).$$

In the above equation, the step size α is proportional to the scale of the optimization problem. The operator $\oplus$ denotes entry-wise multiplication during the random walk process. Levy distribution for large steps is drawn from a random walk, characterized by random steps with infinite variance and an infinite mean. The product $\oplus$ represents the entry-wise walk during these multiplications. Levy flights constitute a stochastic process characterized by a random walk, whereby the random steps are derived from a Levy distribution for substantial movements.

$$Levy \sim u = t^{-\lambda}, \quad 1 < \lambda < 3.$$

The step process of this random walk exhibits a substantial tail and a power-law distribution of step lengths. New solutions are created based on the Levy flight around the optimal solution, which facilitates and expedites the local search.

4.2 Multi-objective function

Objective functions are the most important in the process of optimization. The main aim of the optimization is to minimize the error in the output signal. The objective functions are utilized to tune the controller parameters. In this work, four objective functions are utilized and controller parameters are optimized. Equations (4) to (7) give the mathematical expression of the objective functions where J_1 to J_4 denote Integral absolute error (IAE), Integral time absolute error (ITAE), Integral square error (ISE), and Integral time square error (ITSE), respectively. Where the t, and $e(t)$ are denoted as time and error signal from output. The optimization was done with three scenarios of objective functions single, and combination double & triple.

$$J_1 = IAE = \int_0^\infty |e(t)|dt, \tag{4}$$

$$J_2 = ITAE = \int_0^\infty t \cdot |e(t)|dt, \tag{5}$$

$$J_3 = ISE = \int_0^\infty (e(t))^2 dt, \tag{6}$$

$$J_4 = ITSE = \int_0^\infty t \cdot (e(t))^2 dt. \tag{7}$$

4.3 Optimization results

By utilizing the single and multi-objective functions in CS the following results were obtained. The optimized controller gain parameters are tabulated in Tables 2, 3, and 4 Single, double, and triple objective functions result respectively. While tuning the controller parameters the following fitness convergence is achieved. Figures 6, 7, and 8 represent the single, double, and triple objective functions fitness convergence curves. The average time consumption for computation with different objective functions is shown in Figure 5.

Table 2. OPTIMIZED CONTROLLER GAIN PARAMETERS FOR SINGLE OBJECTIVE FUNCTION

Objective function	K_{p1}	K_{i1}	K_{d1}	K_{p2}	K_{i2}	K_{d2}	**Fitness**
J1	0.968731	0.97253	0.425787	0.66799	0.69982	0.550461	0.02023051
J2	0.772125	0.97966	0.359919	0.6619	0.74813	0.471352	0.09365339
J3	0.950447	0.79059	0.989435	0.74614	0.21825	0.236833	0.00005122
J4	0.998557	0.99014	0.990143	0.15768	0.17481	0.613307	0.00009860

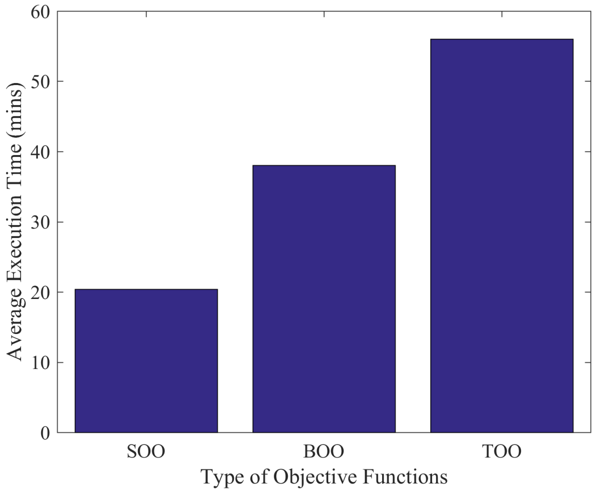

Figure 5. Average execution time

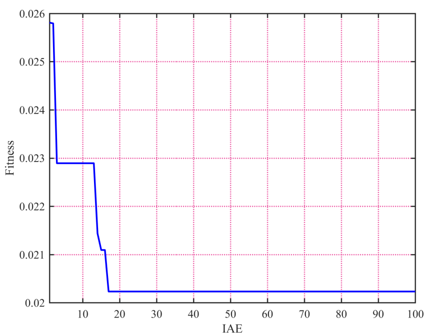

(a) 6a

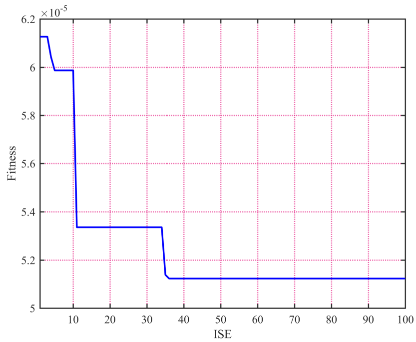

(b) 6b

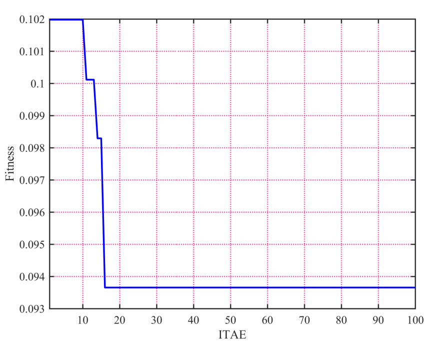

(c) 6c

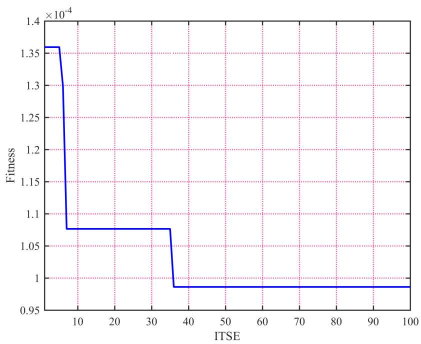

(d) 6d

Figure 6. Convergence curve for single objective functions.

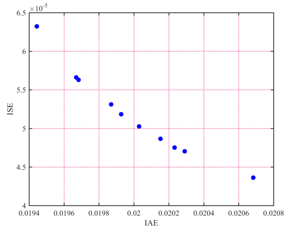

(a) 7a

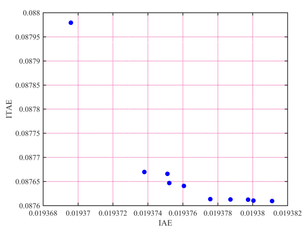

(b) 7b

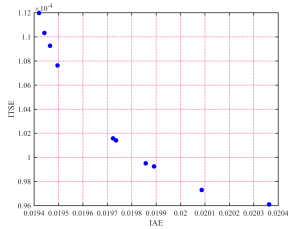

(c) 7c

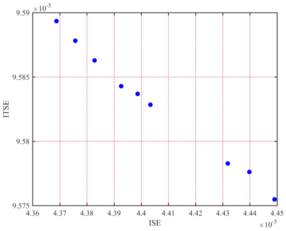

(d) 7d

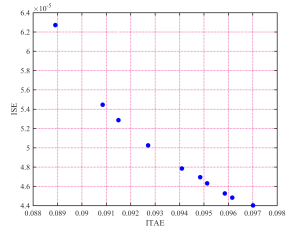

(e) 7e

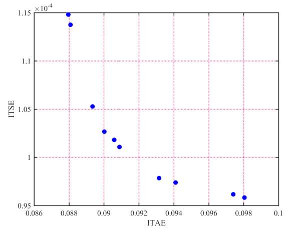

(f) 7f

Figure 7. Convergence curve for double objective functions.

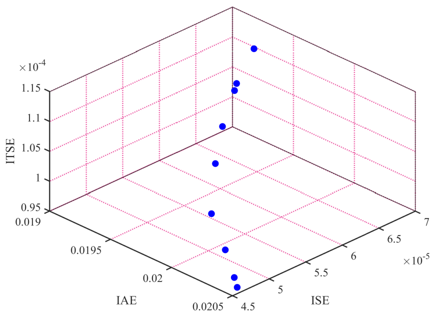

(a) 8a

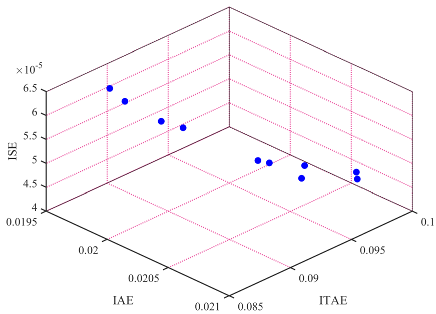

(b) 8b

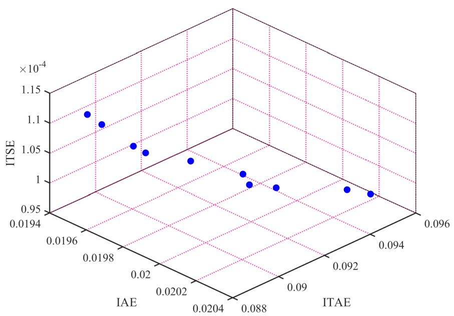

(c) 8c

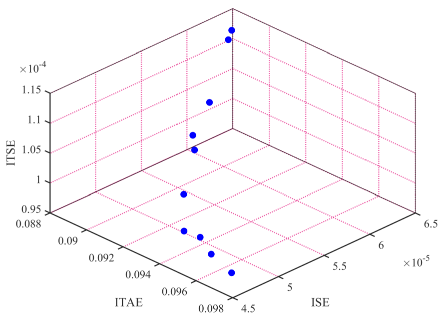

(d) 8d

Figure 8. Convergence curve for triple objective functions.

Table 3. OPTIMIZED CONTROLLER GAIN PARAMETERS FOR DOUBLE OBJECTIVE FUNCTION

Objective function	Objective_min	K_{p1}	K_{i1}	K_{d1}	K_{p2}	K_{i2}	K_{d2}	Fitness	
J1 & J2	IAEmin	0.999898	0.9997872	0.430196	0.981633	0.03982	0.977633	0.019369589	0.087979116
	ITAEmin	0.999667	0.9997659	0.428584	0.997377	0.02332	0.9629127	0.019381111	0.087609389
2*J1 & J3	IAEmin	0.999818	0.9997041	0.474284	0.935424	0.05808	0.644807	0.01944419	0.00006322
	ISEmin	0.995544	0.9997672	0.996764	0.576995	0.03458	0.3378495	0.020683568	0.00004361
2*J1 & J4	IAEmin	0.999665	0.9991443	0.456348	0.979571	0.08186	0.7541447	0.019420506	0.000111969
	ITSEmin	0.999756	0.999328	0.81768	0.940737	0.21991	0.9395463	0.020362967	0.00009609
2*J4 & J3	ITAEmin	0.998282	0.9991197	0.483365	0.915724	0.00761	0.1325223	0.088915882	0.00006271
	ISEmin	0.999315	0.9998115	0.972708	0.970579	0.01503	0.1930226	0.097013373	0.00004401
2*J2 & J4	ITAEmin	0.998526	0.9996387	0.437394	0.924082	0.02571	0.9055836	0.08796038	0.000114801
	ITSEmin	0.99966	0.9992494	0.874236	0.897701	0.24669	0.973135	0.098046549	0.00009582
2*J3 & J4	ISEmin	0.99975	0.9998561	0.996452	0.995169	0.41231	0.9762763	0.00004368	0.00009589
	ITSEmin	0.999854	0.9998645	0.950469	0.992954	0.40963	0.9869591	0.00004449	0.00009575

Table 4. OPTIMIZED CONTROLLER GAIN PARAMETERS FOR TRIPLE OBJECTIVE FUNCTION

Objective function	K_{p1}	K_{i1}	K_{d1}	K_{p2}	K_{i2}	K_{d2}		Fitness	
J1 & J2 & J3	IAEmin	0.98667718	0.99781	0.499141329	0.82419562	0.01883261	0.9132722	0.01959317	0.089288399
	ITAEmin	0.98667718	0.99781	0.499141329	0.82419562	0.01883261	0.9132722	0.01959317	0.089288399
	ISEmin	0.99916074	0.992797679	0.943874059	0.59772864	0.0219842	0.2604135	0.02062169	0.099209552
3*J1 & J2 & J4	IAEmin	0.9988017	0.99955188	0.475774356	0.96550673	0.055074723	0.3598558	0.01945741	0.089191717
	ITAEmin	0.9988017	0.99955188	0.475774356	0.96550673	0.055074723	0.3598558	0.01945741	0.089191717
	ITSEmin	0.99731818	0.999490056	0.749992726	0.96599844	0.228031488	0.5775032	0.02023781	0.09532468
3*J1 & J3 & J4	IAEmin	0.99839316	0.999158856	0.443481671	0.9512848	0.024311388	0.7299798	0.01940895	0.00006614
	ISEmin	0.99941513	0.999743406	0.878226999	0.97148772	0.219148086	0.9797323	0.02048642	0.000045888
	ITSEmin	0.99941513	0.999743406	0.878226999	0.97148772	0.219148086	0.9797323	0.02048642	0.000045888
3*J2 & J3 & J4	ITAEmin	0.99974183	0.999234344	0.460124682	0.96454771	0.02233145	0.5277582	0.08819507	0.00006451
	ISEmin	0.99965401	0.999002355	0.827640563	0.90548769	0.156137926	0.7718504	0.09692577	0.000047039
	ITSEmin	0.99965401	0.999002355	0.827640563	0.90548769	0.156137926	0.7718504	0.09692577	0.000047039

5. Performance analysis

The proposed interlinked nuclear power network is examined for LFC with a multi-objective-based CS–PID controller. An investigation is conducted with one percentage of load demand. The performance is tested in MATLAB2021a Simulink working platform. The effectiveness of the CS algorithm is evaluated in three distinct circumstances.

Scenario 1: Single objective function (SOO).
Scenario 2: Double objective function (BOO).
Scenario 3: Triple objective function (TOO).

5.1 Scenario 1: Single objective function (SOO).

In this section 4, objective functions-based optimization results are analyzed. Figures 9 and 10 represent the frequency analysis of areas 1 and 2 respectively. Figure 11 is a tieline power difference analysis. Table ?? gives the numerical values from Figures 9,10, and 11.

From the result comparison between four objective functions prevailing the performance of the CS algorithm. The ITSE cost function is better than the other three cost functions. ITSE function-based controller settled the frequency oscillation in area 1 quicker than other functions. Not only in the area1, area 2, and tieline power difference also controller over another objective function-based controller.

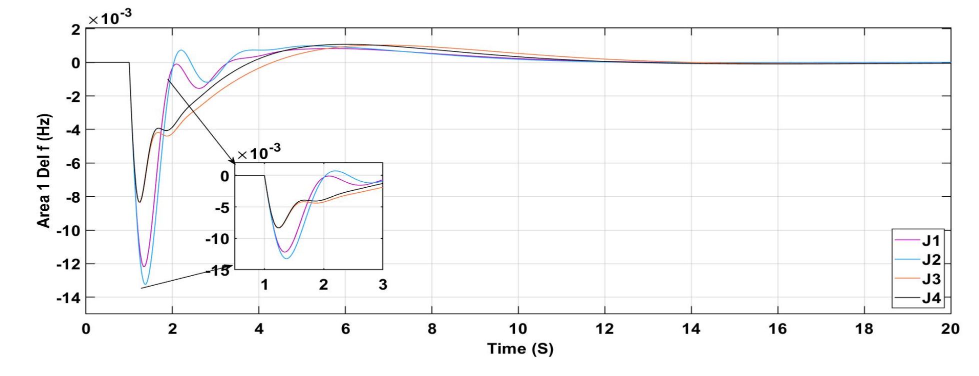

Figure 9. Area$_1$ del f comparison for single objective function.

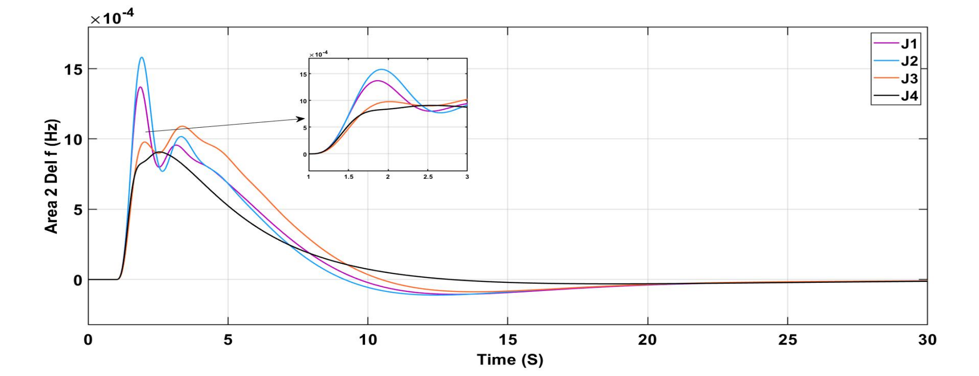

Figure 10. Area$_2$ del f comparison for single objective function.

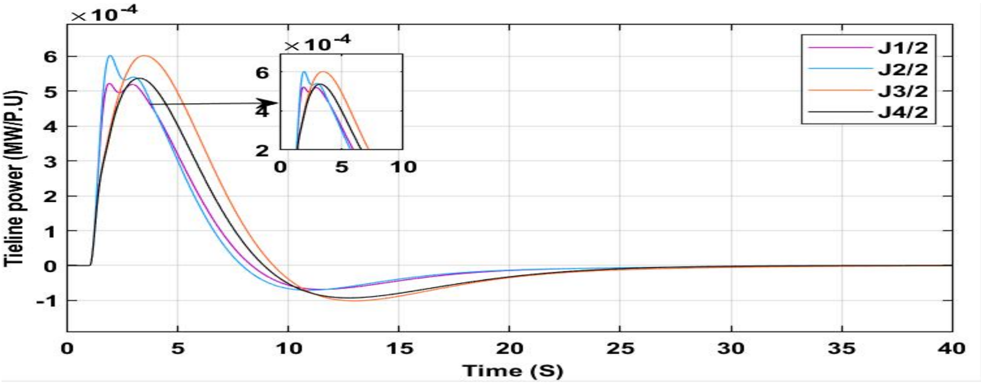

Figure 11. Tieline power difference comparison for single objective function.

5.2 Scenario 2: Double objective function (BOO)

The combined objective functions are utilized to minimize the error from the system frequency. For testing and performance analysis six combinations of double-objective functions were constructed. By using the combinations of objective functions controller gain parame-

Table 5. TIME DOMAIN PARAMETERS FOR SOO

Objective function	First area frequency			Second area frequency			Tie line power		
	TS (S)	PoS (Hz)	PuS (Hz)	TS (S)	PoS (Hz)	PuS (Hz)	TS (S)	PoS (MW/P.U)	PuS (MW/P.U)
J1	13	8.255×10^{-4}	1.218×10^{-2}	35	1.370×10^{-3}	1.053×10^{-4}	35	5.228×10^{-4}	6.835×10^{-5}
J2	11.5	9.827×10^{-4}	1.327×10^{-2}	34	1.583×10^{-3}	1.109×10^{-4}	32	6.031×10^{-4}	7.087×10^{-5}
J3	22	1.027×10^{-3}	8.355×10^{-3}	37	1.091×10^{-3}	8.735×10^{-5}	34	6.024×10^{-4}	1.013×10^{-4}
J4	21	$1.07 4 \times 10^{-3}$	8.326×10^{-3}	45	9.077×10^{-4}	3.061×10^{-5}	30	5.374×10^{-4}	9.283×10^{-5}

ters are optimized. The values are reported in Table 3. The response comparison of area 1 & 2 is given in Figures 12 & 13. The tieline power deviation is given in Figure 14.

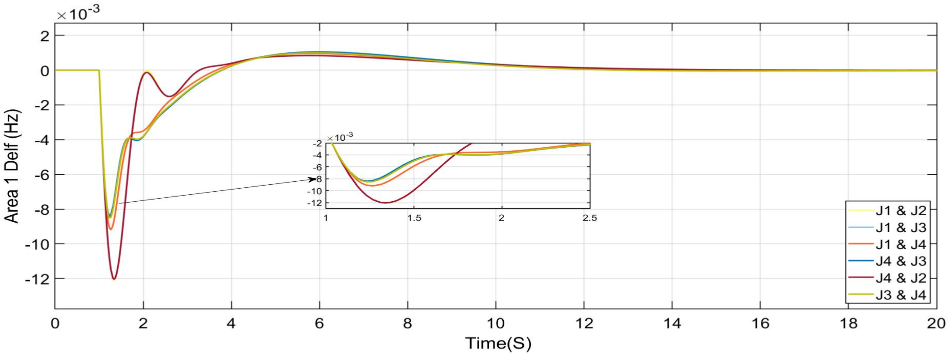

Figure 12. Area 1 del f comparison for the double objective function.

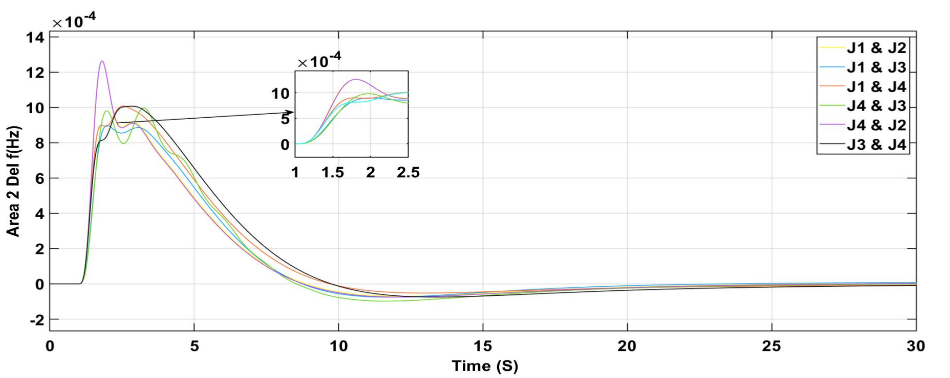

Figure 13. Area 2 del f comparison for double objective function.

The response of the combined objective functions was compared in this section. From the result, we know that the combination of the ITSE objective function with others produced a better transient response over other combinations. As that of the SOO, in BOO also the ITSE objective function responded well. The dominance of ITSE is proved in graphical and numerical. The numerical values from Figures 12 to 14 are in Table 6.

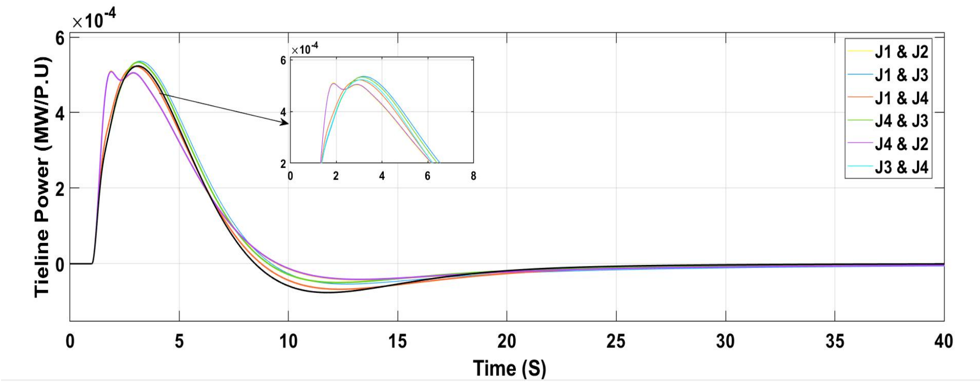

Figure 14. Tieline power difference comparison for the double objective function.

Table 6. TIME DOMAIN PARAMETERS FOR BOO

Objective function	First area frequency			Second area frequency			Tie line power		
	TS (S)	PoS (Hz)	PuS (Hz)	TS (S)	PoS (Hz)	PuS (Hz)	TS (S)	PoS (MW/P.U)	PuS (MW/P.U)
J1 & J2	15	8.336×10^{-4}	1.211×10^{-2}	26	1.263×10^{-3}	6.999×10^{-5}	50	5.112×10^{-4}	4.348×10^{-5}
J1 & J3	13	1.703×10^{-3}	8.326×10^{-3}	24	8.981×10^{-4}	7.515×10^{-5}	50	5.361×10^{-4}	5.398×10^{-5}
J1 & J4	12.5	9.653×10^{-4}	9.190×10^{-3}	40	1.009×10^{-3}	5.175×10^{-5}	35	5.224×10^{-4}	6.775×10^{-5}
J4 & J3	13.5	1.041×10^{-3}	8.423×10^{-3}	27	9.917×10^{-4}	9.766×10^{-5}	42	5.335×10^{-4}	4.986×10^{-5}
J2 &J4	14	8.408×10^{-4}	1.204×10^{-2}	25	1.264×10^{-3}	7.457×10^{-5}	50	5.806×10^{-4}	4.414×10^{-5}
J3 & J4	12	9.999×10^{-4}	8.511×10^{-3}	35	1.073×10^{-3}	7.456×10^{-5}	30	5.234×10^{-4}	7.630×10^{-5}

5.3 Scenario 3: Triple objective function (TOO)

A novel three-objective function combination is worked out in this paper. And the response was compared. For evaluating the CS algorithm's performance. We create and optimize four distinct sets of goal functions for the controller gain parameters. The performance of the three objective function combinations is analyzed in Figures 15 & 16 and the numerical values are reported in Table 7. Figures 15, 16, and 17 indicate that the integration of three-goal

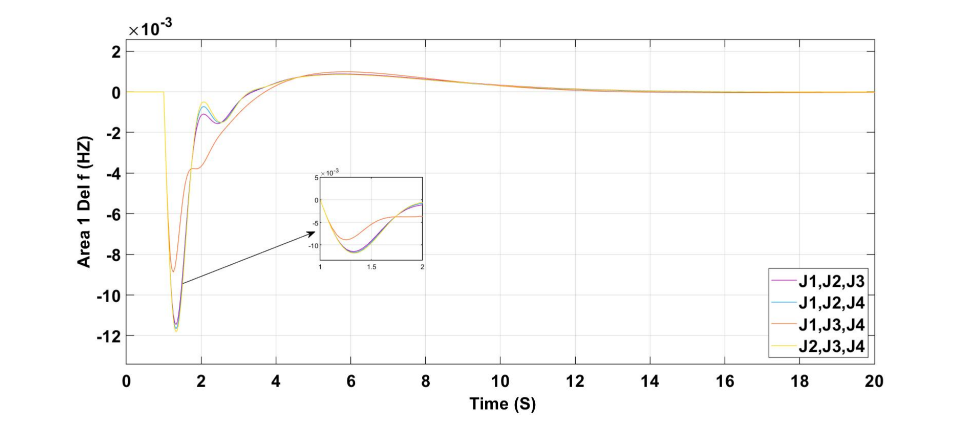

Figure 15. Area 1 del f comparison for the triple objective function.

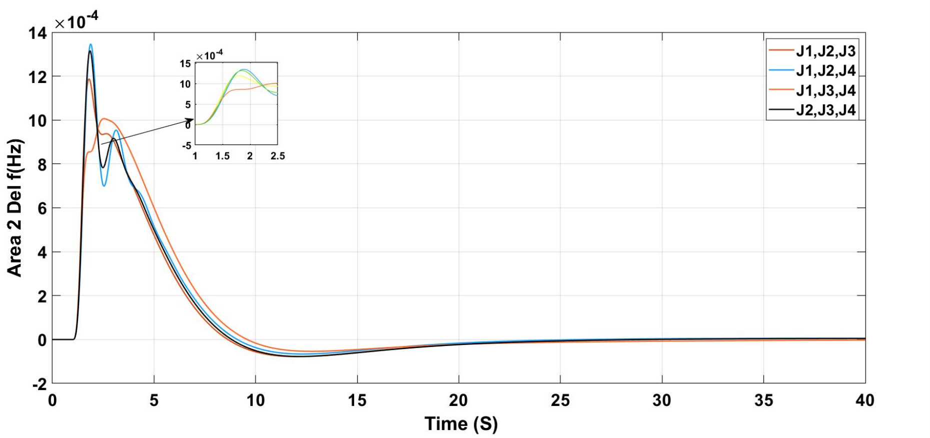

Figure 16. Area 2 del f comparison for the triple objective function.

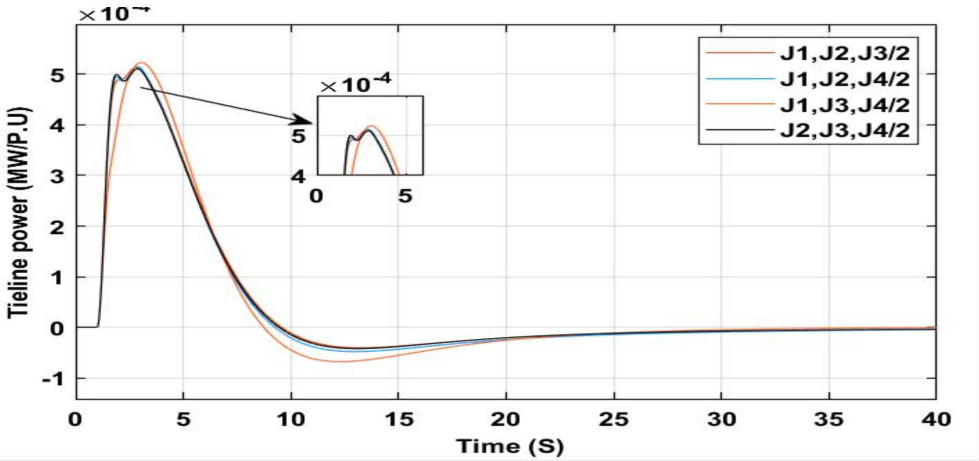

Figure 17. Tieline power difference comparison for the triple objective function.

functions for optimizing the controller gain settings enhances the controller's efficacy in mitigating frequency oscillations. In this circumstance, the combinations using ITSE are executed effectively.

Table 7. TIME DOMAIN PARAMETERS FOR TOO

Objective function	First area frequency			Second area frequency			Tie line power		
	TS (S)	PoS (Hz)	PuS (Hz)	TS (S)	PoS (Hz)	PuS (Hz)	TS (S)	PoS (MW/P.U)	PuS (MW/P.U)
J1 & J2 & J3	14	8.750×10^{-4}	1.151×10^{-2}	25	1.188×10^{-3}	7.791×10^{-5}	50	5.140×10^{-4}	4.615×10^{-5}
J1 & J2 & J4	13	8.562×10^{-4}	1.624×10^{-2}	22	1.347×10^{-3}	6.641×10^{-5}	45	5.134×10^{-4}	4.815×10^{-5}
J1 & J3 & J4	12.5	9.849×10^{-4}	8.856×10^{-3}	36	1.006×10^{-3}	5.391×10^{-5}	33	5.232×10^{-4}	6.812×10^{-5}
J2 & J3 & J4	13	8.154×10^{-4}	1.181×10^{-2}	24	1.316×10^{-3}	7.734×10^{-5}	43	5.114×10^{-4}	4.224×10^{-5}

6. Conclusion

This research evaluates the performance of the Cuckoo Search algorithm for system stability in an interconnected nuclear power station. This study employs four distinct objective functions: IAE, ITAE, ISE, and ITSE. The efficacy of the CS algorithm is evaluated across four distinct goal functions with varying combinations. Each variation of the objective function yields a different outcome. A distinctive outcome from all versions is singular and, when paired with the ITSE function, offers enhanced control responsiveness in both system frequency and tieline power flow. The CS algorithm converged rapidly

Competing Interests None

References

Ali, Hossam Hassan, Ahmed M. Kassem, Mujahed Al-Dhaifallah, and Ahmed Fathy. 2020. Multi-verse optimizer for model predictive load frequency control of hybrid multi-interconnected plants comprising renewable energy. *IEEE Access* 8:114623–114642. ISSN: 2169-3536, https://doi.org/10.1109/access.2020.3004299.

Amir, Mohammad, Mohamed Zaery, Kavita Singh, S. M. Suhail Hussain, and Mohammad A. Abido. 2024. Enhancement of frequency regulation by tfoid controller in hybrid renewable energy with battery storage system-based multi-area microgrids. *IEEE Access* 12:110813–110828. ISSN: 2169-3536, https://doi.org/10.1109/access.2024.3439738.

Basu, M., and A. Chowdhury. 2013. Cuckoo search algorithm for economic dispatch. *Energy* 60 (October): 99–108. ISSN: 0360-5442, https://doi.org/10.1016/j.energy.2013.07.011.

Boopathi, D., K. Jagatheesan, Sourav Samanta, B. Anand, and R. Satheeshkumar. 2023. Energy storage units for frequency management in nuclear generators-based power system. *Energy Storage Technologies in Grid Modernization* (July): 105–134. https://doi.org/10.1002/9781119872146.ch4.

Daneshfar, Fatemeh, and Hassan Bevrani. 2012. Multiobjective design of load frequency control using genetic algorithms. *International Journal of Electrical Power amp; Energy Systems* 42, no. 1 (November): 257–263. ISSN: 0142-0615, https://doi.org/10.1016/j.ijepes.2012.04.024.

Dev, Ark, Sumant Anand, Urvashi Chauhan, Vikash Kr. Verma, and Vineet Kumar. 2023. Frequency regulation in microgrid using sliding mode control with event-triggering mechanism. *Electrical Engineering* 106, no. 3 (December): 3381–3392. ISSN: 1432-0487, https://doi.org/10.1007/s00202-023-02141-6.

Dev, Ark, Bappa Mondal, Vikash Kumar Verma, and Vineet Kumar. 2024. Teaching learning optimization-based sliding mode control for frequency regulation in microgrid. *Electrical Engineering* 106, no. 6 (May): 7009–7021. ISSN: 1432-0487, https://doi.org/10.1007/s00202-024-02422-8.

Dhanasekaran, Boopathi, Saravanan Siddhan, and Jagatheesan Kaliannan. 2020. Ant colony optimization technique tuned controller for frequency regulation of single area nuclear power generating system. *Microprocessors and Microsystems* 73 (March): 102953. ISSN: 0141-9331, https://doi.org/10.1016/j.micpro.2019.102953.

Elgerd, O.I. 1982. *Electric energy systems theory: an introduction.*

Elkasem, Ahmed H. A., Salah Kamel, Mohamed Khamies, and Loai Nasrat. 2024. Frequency regulation in a hybrid renewable power grid: an effective strategy utilizing load frequency control and redox flow batteries. *Scientific Reports* 14, no. 1 (April). ISSN: 2045-2322, https://doi.org/10.1038/s41598-024-58189-2.

Fathy, Ahmed, Anas Bouaouda, and Fatma A. Hashim. 2024. A novel modified cheetah optimizer for designing fractional-order pid-lfc placed in multi-interconnected system with renewable generation units. *Sustainable Computing: Informatics and Systems* 43 (September): 101011. ISSN: 2210-5379, https://doi.org/10.1016/j.suscom.2024.101011.

Fathy, Ahmed, and Ahmed M. Kassem. 2019. Antlion optimizer-anfis load frequency control for multi-interconnected plants comprising photovoltaic and wind turbine. *ISA Transactions* 87 (April): 282–296. ISSN: 0019-0578, https://doi.org/10.1016/j.isatra.2018.11.035.

El-Fergany, Attia A., and Almoataz Y. Abdelaziz. 2014. Capacitor allocations in radial distribution networks using cuckoo search algorithm. *IET Generation, Transmission amp; Distribution* 8, no. 2 (February): 223–232. ISSN: 1751-8695, https://doi.org/10.1049/iet-gtd.2013.0290.

Gashti, Amin, and Adel Akbarimajd. 2020. Designing anti-windup pi controller for lfc of nonlinear power system combined with dsts of nuclear power plant and hvdc link. *Electrical Engineering* 102, no. 2 (January): 793–809. ISSN: 1432-0487, https://doi.org/10.1007/s00202-019-00912-8.

Kalyan, CH. Naga Sai, B. Srikanth Goud, M. Kiran Kumar, Padmanabh Thakur, Mohit Bajaj, and Ramesh C. Bansal. 2023. Squirrel search algorithm based intelligent controller for interconnected power system. *International Journal of Modelling and Simulation* 45, no. 2 (May): 420–440. ISSN: 1925-7082, https://doi.org/10.1080/02286203.2023.2205989.

Khalil, A. Elsawy, Tarek A. Boghdady, M. H. Alham, and Doaa Khalil Ibrahim. 2023. Enhancing the conventional controllers for load frequency control of isolated microgrids using proposed multi-objective formulation via artificial rabbits optimization algorithm. *IEEE Access* 11:3472–3493. ISSN: 2169-3536, https://doi.org/10.1109/access.2023.3234043.

Khalil, A. Elsawy, Tarek A. Boghdady, M.H. Alham, and Doaa Khalil Ibrahim. 2024. A novel multi-objective tuning formula for load frequency controllers in an isolated low-inertia microgrid incorporating pv/wind/fc/bess. *Journal of Energy Storage* 82 (March): 110606. ISSN: 2352-152X, https://doi.org/10.1016/j.est.2024.110606.

Khamies, Mohamed, Gaber Magdy, Mohamed Ebeed Hussein, Fahd A. Banakhr, and Salah Kamel. 2020. An efficient control strategy for enhancing frequency stability of multi-area power system considering high wind energy penetration. *IEEE Access* 8:140062–140078. ISSN: 2169-3536, https://doi.org/10.1109/access.2020.3012119.

Krishna, P. J., V. P. Meena, N. Patnana, A. Mathur, and V. P. Singh. 2022. Grey wolf optimizer-assisted r-method-based weighted minimization for automatic generation control in two-area interconnected power system. *International Journal of Dynamics and Control* 11, no. 4 (October): 1779–1796. ISSN: 2195-2698, https://doi.org/10.1007/s40435-022-01070-9.

Kumar, Sachin, Akhil Gupta, and Ranjit Kumar Bindal. 2024. Load-frequency and voltage control for power quality enhancement in a spv/wind utility-tied system using ga amp; pso optimization. *Results in Control and Optimization* 16 (September): 100442. ISSN: 2666-7207, https://doi.org/10.1016/j.rico.2024.100442.

Kumar, Vineet, Veena Sharma, and Vineet Kumar. 2021. Performance evaluation of hho optimized model predictive controller for avr system and its comparison with conventional controllers. In *Machine learning, advances in computing, renewable energy and communication,* 151–159. Springer Singapore, August. ISBN: 9789811623547, https://doi.org/10.1007/978-981-16-2354-7_14.

Mamta, V. P. Singh, Akanksha V. Waghmare, Veerpratap P. Meena, Francesco Benedetto, and Tarun Varshney. 2024. Rank exponent method based optimal control of agc for two-area interconnected power systems. *IEEE Access* 12:35571–35585. ISSN: 2169-3536, https://doi.org/10.1109/access.2024.3373043.

Masikana, S. B., Gulshan Sharma, Sachin Sharma, and Emre undefinedelik. 2024. Frequency regulation in solar pv-powered thermal power system using fpa-pid controller through upfc and rfb. *Electrical Engineering* 107, no. 7 (May): 8665–8677. ISSN: 1432-0487, https://doi.org/10.1007/s00202-024-02417-5.

Metwally, M. A., M. A. Ali, S. A. Kutb, and F. M. Bendary. 2024. A genetic algorithm for optimum design of pid controller in multi-area load frequency control for egyptian electrical grid. Http://www.ijert.org ISSN: 2278-0181, *International Journal of Engineering Research & Technology (IJERT).*

Misaghi, Mojgan, and Mahdi Yaghoobi. 2019. Improved invasive weed optimization algorithm (iwo) based on chaos theory for optimal design of pid controller. *Journal of Computational Design and Engineering* 6, no. 3 (January): 284–295. ISSN: 2288-5048, https://doi.org/10.1016/j.jcde.2019.01.001.

Mishra, Dillip K., Asit Mohanty, and Prakash K. Ray. 2023. An optimal frequency regulation in interconnected power system through differential evolution and firefly algorithm. *Soft Computing* 28, no. 1 (May): 593–606. ISSN: 1433-7479, https://doi.org/10.1007/s00500-023-08314-6.

Murugesan, D, K Jagatheesan, Anand J Kulkarni, and Pritesh Shah. 2023. A socio inspired technique in nuclear power plant for load frequency control by using cohort intelligence optimization-based pid controller. In *Renewable energy optimization, planning and control,* 1–12. Springer Nature Singapore. ISBN: 9789811989636, https://doi.org/10.1007/978-981-19-8963-6_1.

Naidu, K., V. Terzija, A.H.A. Bakar, and H. Mokhlis. 2014. Comparative performance analysis of firefly algorithm for load frequency control in automatic generation control of interconnected reheat thermal power system. In *3rd iet international conference on clean energy and technology (ceat) 2014,* 24 (6 .)–24 (6 .) Institution of Engineering / Technology. https://doi.org/10.1049/cp.2014.1471.

Namdeo, Rishika, Manjaree Pandit, and Nikhil Paliwal. 2023. Sine cosine algorithm-based fractional-order pid controller for load frequency control in a single area nuclear power plant. In *2023 7th international conference on* *computer applications in electrical engineering-recent advances (cera),* 1–5. IEEE, October. https://doi.org/10.1109/cera59325.2023.10455393.

OECD International Energy Agency. 2023. *World energy outlook 2023.*

Paliwal, Nikhil, Laxmi Srivastava, Manjaree Pandit, and Poonam Singh. 2021. Jaya algorithm-based load frequency control in nuclear power plant incorporating energy storage unit. In *Artificial intelligence and sustainable computing,* 239–252. Springer Singapore, July. ISBN: 9789811612206, https://doi.org/10.1007/978-981-16-1220-6_21.

Qu, Zhengwei, Waqar Younis, Xianglin Liu, Abdul Khalique Junejo, Sulaiman Z. Almutairi, and Peng Wang. 2024. Optimized pid controller for load frequency control in multi-source and dual-area power systems using pso and ga algorithms. *IEEE Access* 12:186658–186678. ISSN: 2169-3536, https://doi.org/10.1109/access.2024.3445165.

Qu, Zhengwei, Waqar Younis, Yunjing Wang, and Popov Maxim Georgievitch. 2024. A multi-source power system's load frequency control utilizing particle swarm optimization. *Energies* 17, no. 2 (January): 517. ISSN: 1996-1073, https://doi.org/10.3390/en17020517.

Yang, Xin-She, and Suash Deb. 2010a. Cuckoo search via levy flights. arXiv. https://doi.org/10.48550/ARXIV.1003.1594.

Yang, Xin-She, and Suash Deb. 2010b. Engineering optimisation by cuckoo search, https://doi.org/10.48550/ARXIV.1005.2908.

Yang, Xin-She, and Suash Deb. 2013. Multiobjective cuckoo search for design optimization. *Computers amp; Operations Research* 40, no. 6 (June): 1616–1624. ISSN: 0305-0548, https://doi.org/10.1016/j.cor.2011.09.026.

Ye, Yidie, Amil Daraz, Abdul Basit, Irfan Ahmed Khan, and Salman A. AlQahtani. 2024. Cascaded fractional-order controller-based load frequency regulation for diverse multigeneration sources incorporated with nuclear power plant. Edited by Yogendra Arya. *International Journal of Energy Research* 2024, no. 1 (January). ISSN: 1099-114X, https://doi.org/10.1155/2024/7939416.

Younis, Waqar, Muhammad Zubair Yameen, Abu Tayab, Hafiz Ghulam Murtza Qamar, Ehab Ghith, and Mehdi Tlija. 2024. Enhancing load frequency control of interconnected power system using hybrid pso-aha optimizer. *Energies* 17, no. 16 (August): 3962. ISSN: 1996-1073, https://doi.org/10.3390/en17163962.

Zhao, Weiguo, Tiancong Shi, Liying Wang, Qingjiao Cao, and Hongfei Zhang. 2021. An adaptive hybrid atom search optimization with particle swarm optimization and its application to optimal no-load pid design of hydro-turbine governor. *Journal of Computational Design and Engineering* 8, no. 5 (August): 1204–1233. ISSN: 2288-5048, https://doi.org/10.1093/jcde/qwab041.